

Published in final edited form as:

*Biosens Bioelectron.* 2011 March 15; 26(7): 3297–3302. doi:10.1016/j.bios.2011.01.001.

## Highly sensitive single polyaniline nanowire biosensor for the detection of immunoglobulin G and myoglobin

Innam Lee<sup>a</sup>, Xiliang Luo<sup>b</sup>, Xinyan Tracy Cui<sup>b</sup>, and Minhee Yun<sup>a,b,\*</sup>

<sup>a</sup>University of Pittsburgh, Department of Electrical and Computer Engineering, Pittsburgh, PA 15261, USA

<sup>b</sup>University of Pittsburgh, Department of Bioengineering, Pittsburgh, PA 15260, USA

### Abstract

A single polyaniline (PANI) nanowire-based biosensor was established to detect immunoglobulin G (IgG) and myoglobin (Myo), which is one of the cardiac biomarkers. The single PANI nanowires were fabricated via an electrochemical growth method, in which single nanowires were formed between a pair of patterned electrodes. The single PANI nanowires were functionalized with monoclonal antibodies (mAbs) of IgG or Myo via a surface immobilization method, using 1-ethyl-3-(3-dimethylaminopropyl) carbodiimide (EDC), and N-Hydroxysuccinimide (NHS). The functionalization was then verified by Raman spectroscopy and fluorescence microscopy. The target proteins of IgG and Myo were detected by measuring the conductance change of functionalized single PANI nanowires owing to the capturing of target proteins by mAbs. The detection limit was found to be 3 ng/mL for IgG and 1.4 ng/mL for Myo. No response was observed when single nanowires were exposed to a non-specific protein demonstrating excellent specificity to expected target detection. Together with the fast response time (a few seconds), high sensitivity, and good specificity, this single PANI nanowire-based biosensor shows great promise in the detection of cardiac markers and other proteins.

### Keywords

Polyaniline nanowire; Biosensing; Immunoglobulin G; Myoglobin; Surface immobilization

## 1. Introduction

Various biosensors based on new materials have been developed that improve the resolution of detection, cost efficiency, and portability for diagnosis of diseases (Masson et al. 2006). The diagnosis of cardiovascular disease, a leading cause of death, requires the detection of cardiac biomarkers such as myoglobin (Myo), cardiac troponin I (cTnI), creatine kinase-MB (CK-MB), and B-type natriuretic peptide (BNP) (Hamm 2001). Many research groups have employed methods such as fluorescence absorbance (Darain et al. 2009), nanomechanical

© 2011 Elsevier B.V. All rights reserved.

\*Corresponding Author. Tel: +1-412-648-8988; Fax: +1-412-624-8003. miy16@pitt.edu (M. Yun).

**Publisher's Disclaimer:** This is a PDF file of an unedited manuscript that has been accepted for publication. As a service to our customers we are providing this early version of the manuscript. The manuscript will undergo copyediting, typesetting, and review of the resulting proof before it is published in its final citable form. Please note that during the production process errors may be discovered which could affect the content, and all legal disclaimers that apply to the journal pertain.

### Appendix A. Supplementary data

Supplementary data associated with this article can be found in the online version, at doi:

cantilever array (Arntz et al. 2003), and surface-enhanced resonance Raman scattering (Cotton et al. 1980) for cardiac biomarker sensing. In current technology, sensing of cardiac biomarkers requires substantial time due to the slow response of measurement methods such as sandwich ELISA (Ishii et al. 1997) and sample preparation from human serum. To achieve label-free and highly sensitive detection, nanomaterials such as nanowires, nanoparticles, and carbon nanotubes are very appealing due to their fast transport of electrons in one-dimensional structure (Wanekaya et al. 2006). In this regard, nanowire-based biosensors have been widely investigated because of the advantages of nanowires such as high sensitivity as a result of the high surface to volume ratio, low power consumption, and the potential for miniaturization of application devices (Gooding 2006; Patolsky et al. 2006). To date, nanowire-based sensors have demonstrated good reproducibility, portability, and label-free detection (Ishikawa et al. 2009).

In order to utilize nanowires for biosensors, functionalization of the nanowire is one of the essential steps in satisfying requirements such as high resolution and good specificity of target detection. Several biomolecular functionalization methods have been developed including entrapment of bio-receptors, conjugation of biotin-streptavidin, and surface immobilization of monoclonal antibodies (mAbs) (Muhammad-Tahir and Alocilja 2003; Sangodkar et al. 1996). Among these functionalization methods, the surface immobilization method is easy and efficient as many biomolecules can be covalently coupled on the surface area of nanowires. Furthermore, many nano-biosensors have been developed by employing inorganic nanowires or carbon nanotubes through the chemical bonding of bio-receptors to their surfaces (Tang et al. 2006). However, surface immobilization of inorganic nanowire often requires multiple steps of chemical reaction due to its low reactivity to biomolecules (Luo et al. 2006). In this regard, organic nanowires, such as polyaniline (PANI) and polypyrrole (Ppy), are very promising candidate materials for biosensor applications because they can be functionalized relatively easily because of the tunability of the doping ratio on the amine group to provide the functional group to biomolecules (Ahuja et al. 2007).

Conducting polymers such as PANI and Ppy have been fabricated into thin films, powders, nanoparticles, or nanowires and utilized for chemical or biosensors taking advantage of their wide range of conductivity, ease of synthesis, environmental stability, and biocompatibility (Adhikari and Majumdar 2004). Although various biosensors based on conducting polymer nanowires have been developed, many of them only use bundled nanowires or nanowire arrays, which limit the development of a single nanowire application (Kwon et al. 2010). In this regard, the promising direction is in the use of a single nanowire or limited number from selected nanowires in order to achieve high sensitivity and constant performance of biosensors. However, due to the difficulty of handling a single nanowire, only a few biosensors based on a single nanowire have been developed (Yun et al. 2004), and they exhibited poor reproducibility as the single nanowire in those biosensors are randomly positioned (Gao et al. 2007).

In this research, we have demonstrated a novel conductometric biosensor based on a functionalized single PANI nanowire to detect immunoglobulin G (IgG) and Myo. A conductometric nanowire biosensor provides fast detection, good specificity, and high sensitivity induced through the conductance change of nanowire without tedious processes such as sample preparation, separation, or some signal filtering process required in amperometric biosensors (Muhammad-Tahir and Alocilja 2003; Wang et al. 2005). Single PANI nanowires were fabricated via an electrochemical growth method, which deposited PANI along a nanochannel bridged on a pair of patterned electrodes with *in situ* electropolymerization. Unlike other nanowire fabrication methods such as electrochemical deposition through anodic aluminum oxide (AAO) template or electrospinning, which generates bundles of nanowires and requires a post-assembly for device application, an

electrochemical growth method enables the direct fabrication of a single site-specific nanowire. After using 1-ethyl-3-(3-dimethylaminopropyl) carbodiimide (EDC) and N-Hydroxysuccinimide (NHS) (Dong et al. 2008), the fabricated single PANI nanowires were functionalized with IgG and Myo mAbs. The single PANI nanowire biosensor shows high sensitivity with a very low detection limit and good sensing linearity in response to broad concentration ranges of target proteins such as IgG and Myo. The proposed method represents a novel, robust, and simple way to establish single PANI nanowire biosensor chips. The same mechanism will be applied to different conducting polymer nanowires and various sensing targets.

## 2. Experimental

### 2.1. Reagents

Aniline ( $\geq 99.5\%$ ), EDC, NHS, and bovine serum albumin (BSA) were purchased from Sigma Aldrich. Phosphate buffer solution (PBS, pH 7.4) was used to prepare the solutions of EDC (0.2 M), NHS (0.2 M), BSA (100 ng/mL – 2 mg/mL), IgG (1 ng/mL – 10  $\mu\text{g/mL}$ ), and Myo (1 ng/mL – 10  $\mu\text{g/mL}$ ). Goat anti-rabbit IgG mAbs and IgG protein were purchased from Invitrogen. Myo mAbs and human cardiac Myo were purchased from Abcam to demonstrate a single PANI nanowire-based cardiac biosensor.

### 2.2. Preparation of the single PANI nanowire via electrochemical growth method

The single PANI nanowire was grown using electropolymerization of ionized aniline monomers in a nanochannel. Pre-patterned Au electrodes and nanochannels were built up lithographically using an e-beam evaporator (VE-180, Thermionics) and an e-beam lithography machine (e-line, Raith) as shown in Fig. S1A (See supplementary data). The width of the nanochannel is 100 nm and the distance between two electrodes is 5  $\mu\text{m}$ . Single PANI nanowire growth was achieved using a probe station and a semiconductor device analyzer (B1500A, Agilent); a 0.4  $\mu\text{L}$  aniline solution (0.01 M in 0.1 M HCl) was dropped covering the nanochannel while a static current was applied between the two metal electrodes as illustrated in Fig. S1B, explained in detail elsewhere (Lee et al. 2008). The measured voltage between the two metal electrodes was monitored in the process of nanowire growth via a semiconductor device analyzer. The nanowire growth was completed when the voltage across the nanowire dropped to the order of microvolt, indicating a short circuit had been achieved. The fabricated single PANI nanowires were immersed in acetone for 5 min and rinsed with deionized water for 1 min. This step was performed to remove the polymethylmethacrylate (PMMA) layer and coagulate the nanowires by dehydration of the backbone of the PANI (Pomfret et al. 2000). The fabricated single PANI nanowire is illustrated connecting a pair of electrodes as shown in Fig. S1C.

### 2.3. Functionalization of the single fabricated PANI nanowire

In order to develop a biosensor based on the single PANI nanowire, surface immobilization of the nanowire was employed using mAbs of target proteins, EDC, and NHS. This method involves coupling mAbs to the single PANI nanowire, with EDC/NHS facilitating the covalent bonding. In this research, the mixture solution of EDC/NHS (0.2/0.2 M) with mAbs of target proteins was dropped on the top of single PANI nanowires and incubated for 3 h at room temperature in a dark area. Then these single PANI nanowires were washed using a PBS and deionized water to eliminate un-immobilized mAbs. The concentrations of mAbs were varied from 50  $\mu\text{g/mL}$ , 100  $\mu\text{g/mL}$ , and 200  $\mu\text{g/mL}$  for optimizing the functionalization condition. The covalently coupled mAbs on the single PANI nanowire play roles of receptors in detecting target proteins and inducing the change of conductance in the single nanowire after binding the target proteins to mAbs. After surface immobilization, the single PANI nanowires were soaked in a high concentration of BSA (2

mg/mL) for 30 min to block the non-specific protein interactions to the biosensor. For a specific sensing test, IgG mAbs were employed to sense the IgG proteins. IgG sensing development provides fundamental mechanism of the single PANI nanowire biosensor thorough characterization and optimization with relatively lower cost. The findings for single PANI nanowire biosensing can then be applied to sensing other proteins such as Myo in this work. Therefore, we used Myo mAbs for cardiac biomarker sensing. Fig. S1D illustrates a functionalized single PANI nanowire with mAbs for the biosensor.

In order to verify the surface immobilization on the single PANI nanowire, the Texas Red labeled IgG mAbs were functionalized on the single PANI nanowires, and those nanowires were imaged under a fluorescence microscope (Axioskop 2 MAT, Carl Zeiss) using a camera (AxioCamMRC5, Carl Zeiss) attached to the scope and software AxioVision Rel 4.2. Additionally, scanning electron microscopy (SEM, E-Line, Raith) and Raman spectroscopy (inVia, Renishaw) were used to study the change of surface morphology and the chemical structure on the nanowires before and after the functionalization, respectively.

#### 2.4. Measurement of conductance change to sense target proteins

The functionalized single PANI nanowires were used to detect target proteins of IgG and Myo in broad range from a single ng/mL to a single  $\mu\text{g/mL}$  by measuring conductance changes of the functionalized single PANI nanowires at room temperature ( $23 \pm 2$  °C) due to similarity to practical case. The bio-activity of antigen or antibody is dependent to the change of temperature. But, it is ignorable that the biosensing is carried out in small variance of temperature like  $\pm 2$  °C (Ruben et al. 1977). The conductance changes due to the binding of target proteins were measured with a semiconductor device analyzer, which was connected to the measurement box where the functionalized single PANI nanowires biosensors were mounted. The measurement was carried out applying a static current of 50 nA with a sampling ratio of 2 Hz. A baseline of the conductance was first obtained by measuring the conductance values from the functionalized single nanowire in PBS solution. The conductance changes between initial baseline in PBS and measured conductance values at specific concentrations of target proteins were used as the sensing signal. It was possible to develop the highly sensitive biosensor due to the resolution of the single nS scale of the semiconductor device analyzer and the customized aluminum measurement box to shield external noise.

### 3. Results and Discussions

#### 3.1. Functionalization of the single PANI nanowire

In order to verify functionalization on the single PANI nanowire, several techniques were employed using characterization samples in this research. SEM images show the change of morphology from the before and after functionalization of single PANI nanowires, respectively, while destroying biosensor functionality. The non-functionalized single PANI nanowire shows a width of 105.4 nm with a smooth and clean surface as shown in Fig. 1A. After the functionalization, some particles on the nanowire were clearly observed in Fig. 1B. The size of those particles was measured from 10 nm to 15 nm in diameter. In addition, the surface of the functionalized single PANI nanowire became rougher than the non-functionalized one as compared in Fig. 1A and Fig. 1B. Therefore, it is speculated that those particles are the immobilized IgG mAbs, where the average size of the IgG mAbs are consistent with the range of SEM measurement, or their aggregations. Similar results were also reported by other research groups (Kwon et al. 2010; Zhang et al. 2001).

For easy characterization, the functionalization of PANI with IgG mAbs was first tested on PANI thin films. The functionalized PANI thin film with fluorescently labeled IgG mAbs

was observed under a fluorescence microscope. It is an effective method to identify the firmly immobilized mAbs on expected areas such as only PANI thin film or nanowires using the fluorescent lights tagged on IgG mAbs (See Fig S2A). As shown in Fig. S2A, fluorescent dots are evenly distributed on the PANI thin film surface indicating that the mAbs were successfully immobilized on the PANI thin films. Further characterizations of the thin film structure were performed using Raman spectroscopy as shown in Fig. S2B. The Raman spectrum of the non-functionalized PANI thin film in this work has typical peaks of doped PANI on  $1590\text{ cm}^{-1}$  (C=C bonding),  $1480\text{ cm}^{-1}$  (C=N bonding),  $1431\text{ cm}^{-1}$  (C-C stretching),  $1220\text{ cm}^{-1}$  (C-N stretching),  $1165\text{ cm}^{-1}$  (in-plane C-H bending),  $840\text{ cm}^{-1}$  (Amine deform),  $779\text{ cm}^{-1}$  (Ring deform), and  $750\text{ cm}^{-1}$  (Imine deform). Those peaks are characteristics of a doped conducting PANI structure (Zhang et al. 2005). The spectrum of the PANI thin film structure after functionalization presents new peaks at  $1638\text{ cm}^{-1}$  and  $1240\text{ cm}^{-1}$ , which represent the chemical structure of Amide I ( $1638\text{ cm}^{-1}$ ) and Amide III ( $1240\text{ cm}^{-1}$ ) in IgG mAbs (Painter and Koenig 1975). Hence the comparison of Raman spectra clearly shows the existence of IgG mAbs on the functionalized PANI thin film structure.

Next, the functionalized single PANI nanowires with IgG mAbs were characterized using fluorescence microscopy and Raman spectroscopy. As shown in Fig. 1C, the red fluorescence is only seen on the region of the single PANI nanowire between the electrodes. The fluorescence was emitted from the fluorescent dyes on IgG mAbs that were immobilized on the surface of the single PANI nanowire via the functionalization process. We found that IgG mAbs emit strong enough fluorescence despite the very small size of the single nanowire, because the IgG mAbs agglomerate together as shown in the SEM image. Raman spectra before and after the functionalization of the single PANI nanowires are also shown in Fig. 1D. The single PANI nanowire structure and the thin film results are similar. The functionalized single PANI nanowire structure also shows peaks at  $1240\text{ cm}^{-1}$  and  $1638\text{ cm}^{-1}$  as compared to the Raman spectrum of the PANI thin film structure. However, the Amide III band of IgG mAbs at  $1240\text{ cm}^{-1}$  in the single PANI nanowire has a relatively weak peak due to the strong intensity of the single PANI nanowire at  $1220\text{ cm}^{-1}$  after functionalization. These characterizations confirmed the successful immobilization of IgG mAbs on the single PANI nanowire. Therefore, in this research, we employed this functionalization method to develop a single PANI nanowire biosensor for the detection of IgG and Myo.

### 3.2. IgG biosensing

The detection of proteins such as IgG and Myo on the single PANI nanowire biosensor is based on measuring the conductance changes of the single nanowires to target proteins and their different concentrations. The IgG protein was first tested to demonstrate the feasibility of the single PANI nanowire biosensor using a conductometric mechanism in this research.

Various tests on non-functionalized and functionalized PANI nanowire biosensors for IgG detection are presented in Fig. 2. The non-functionalized PANI nanowire biosensor shows no changes of conductance to PBS (pH 7.4), BSA ( $10\text{ }\mu\text{g/mL}$ ), and IgG, which indicates non-response to PBS and proteins to identify non-sensibility of the non-functionalized PANI nanowire, as shown in Fig. 2A. In Fig. 2B, for the functionalized single PANI nanowire biosensor with IgG mAbs, its conductance increases with the injection of PBS due to the change of the surface charge induced from the net electrical charge of IgG mAbs. As can be seen Fig. 2B, there is no response to injected BSA ( $50\text{ ng/mL}$ ) and a distinct response to IgG ( $33\text{ ng/mL}$ ) from BSA injection, showing a good specificity of the biosensor to IgG. In Fig. 2C, in sensing different concentrations of IgG, the functionalized single PANI nanowire with  $100\text{ }\mu\text{g/mL}$  IgG mAbs shows stepwise changes along different concentrations of IgG

detecting the lowest level of 5 ng/mL IgG and non-response to high concentration of BSA (5  $\mu\text{g/mL}$ ).

The conductometric sensing mechanism of the single PANI nanowire biosensor, where the nanowire is a p-type, can be explained by field-effect behavior (Chua et al. 2009; Gerard et al. 2002; Lin et al. 2010). When negative surface charges are applied to a p-type nanowire, its conductance is increased with accumulation of the major carrier in the nanowire. The IgG protein has a weak negative charge in PBS (pH 7.4) due to its isoelectric point (pI) value of 7.2. The single PANI nanowire biosensor for IgG sensing shows the increase of conductance detecting IgG as demonstrated in this work. In addition to the injection of target proteins or PBS, the conductance change of the functionalized PANI nanowire increases or decreases according to the net charge of the injected solution. With regard to the sensing reliability, the conductometric sensing mechanism of the single PANI nanowire biosensor provides steady sensing performance with equilibrium reaction between mAbs and proteins (Gerard et al. 2002). Furthermore, the conductometric sensing mechanism has advantages not to require reference electrode, to work in low voltage, and to minimize interference with blocking of the functionalized surface (Nyamsi Hendji et al. 1994; Tang et al. 2011).

We further investigated the effect of various IgG mAbs concentrations (50  $\mu\text{g/mL}$ , 100  $\mu\text{g/mL}$ , and 200  $\mu\text{g/mL}$ ) by studying the sensitivity of the single PANI nanowire biosensor as well as optimizing the functionalization condition as plotted in Fig. 2D, with a percentage (%) scale for sensitivity and a log scale for IgG concentration. The performance of the single PANI nanowire biosensor is determined by its sensitivity ( $\Delta S/S_0$ ;  $\Delta S$ : absolute value of conductance change,  $S_0$ : initial conductance in PBS). The single PANI nanowire biosensor using IgG mAbs of 50  $\mu\text{g/mL}$  shows ~40% change at low IgG concentration (10 ng/mL). However, the sensitivity saturates at ~50% as soon as reaching the high IgG concentration (300 ng/mL – 2  $\mu\text{g/mL}$ ). On the other hand, it is observed that the single PANI nanowire using IgG mAbs of 100  $\mu\text{g/mL}$  shows noticeable change along a wide range of IgG concentrations (3 ng/mL – 3  $\mu\text{g/mL}$ ); better than from the functionalization condition with IgG mAbs of 50  $\mu\text{g/mL}$ . Additionally, the conductance change can be as high as 300% at the highest IgG concentration (3  $\mu\text{g/mL}$ ). The single PANI nanowire biosensor using IgG mAbs of 200  $\mu\text{g/mL}$  has relatively low sensitivity and shows a small difference between the low concentration range (5 – 100 ng/mL) and high concentration range (100 ng/mL – 3  $\mu\text{g/mL}$ ) of IgG. Based on this observation, it is concluded that immobilization with IgG mAbs of 100  $\mu\text{g/mL}$  provides the most effective number of receptors than other mAbs concentrations, avoiding insufficiency of detection in IgG mAbs of 50  $\mu\text{g/mL}$  or insensitivity that might be caused by agglomeration of mAbs from excessive immobilization with IgG mAbs of 200  $\mu\text{g/mL}$ . Therefore, the optimal functionalization condition of the single PANI nanowire biosensor for IgG detection is IgG mAbs of 100  $\mu\text{g/mL}$ , which shows high sensitivity and good sensing linearity from a single ng/mL scale up to a  $\mu\text{g/mL}$  scale. Proof-of-concept work done with IgG was applied to the single PANI nanowire biosensor for practical application such as Myo sensing, which is one of the most important cardiac biomarkers for cardiovascular disease diagnosis.

### 3.3. Myo sensing

The Myo mAbs were immobilized on the single PANI nanowires using the same method introduced above. The conductance changes of the single PANI nanowire biosensor for Myo detection were measured in PBS, BSA, and Myo solution as shown in Fig. 3A. The single PANI nanowire biosensor shows no response to high concentration of BSA (500 ng/mL) but a clear conductance change to Myo (1.4 ng/mL), demonstrating a good specificity and high sensitivity to Myo. The Myo solution in PBS (pH 7.4) has a weak negative charge due to its pI value of 6.85. Therefore, the captured Myo proteins by mAbs result in negative surface charges on ptype nanowire, and increase the conductance as shown in Fig. 3A. The wide

range of Myo concentrations, from 1.4 ng/mL to 2.5  $\mu$ g/mL, was tested on the single PANI nanowire biosensor using Myo mAbs. It is shown that the single PANI nanowire biosensor measures conductance change detecting Myo in the whole range of Myo concentration (5 ng/mL – 2.5  $\mu$ g/mL) as shown in Fig. 3B. Because the normal Myo concentration ranges in human serum are from 6 ng/mL to 85 ng/mL (de Winter et al. 1995), the single PANI nanowire biosensor in this research is sensitive enough for the real application diagnosis. Similar to the IgG biosensor, the different concentrations of Myo mAbs (100  $\mu$ g/mL and 200  $\mu$ g/mL) were studied to obtain the optimal condition of single PANI nanowire biosensor for Myo detection as shown in Fig. 3C. The single PANI nanowire biosensors using Myo mAbs of 100  $\mu$ g/mL show higher sensitivity and better sensing linearity in the detection range of Myo proteins (1.4 ng/mL – 2.5  $\mu$ g/mL) than the biosensor using Myo mAbs of 200  $\mu$ g/mL. Under the optimized functionalization condition (Myo mAbs of 100  $\mu$ g/mL) in this research, the functionalized PANI nanowire shows uniformly attached Myo mAbs on its surface, as shown in the SEM image (Fig. S3). Therefore, for the detection of Myo via single PANI nanowire biosensors, we have observed good sensing specificity, linear sensing profile, and high sensitivity as demonstrated in Fig. 3. Furthermore, these biosensors developed in this research show a fast response time of a few seconds and low detection limit (1.4 ng/mL), which is sufficient for Myo detection in human serum.

#### 4. Conclusion

A single PANI nanowire biosensor has been fabricated through a site-specific electrochemical growth method and surface immobilization mAbs with the assistance of EDC/NHS in this research. The EDC/NHS assists to form strong covalent bonds between mAbs and PANI nanowire easily and effectively. The proposed biosensors based on single PANI nanowires exhibited good specificity and high sensitivity towards the detection of IgG and Myo. Moreover, the single PANI nanowire biosensor shows the feasibility of label-free detection with a fast response time of a few seconds for various biosensor applications. It is expected that the surface immobilization for single PANI nanowires assisted by EDC/NHS will be employed in other mAbs of various protein detection tests such as cardiac markers or cancer markers in the future.

#### Supplementary Material

Refer to Web version on PubMed Central for supplementary material.

#### Acknowledgments

Financial support for this research was provided by the National Science Foundation (NSF, Grant ECCS 0824035) and support from the National Institutes of Health (NIH, NIH 1R21EB008825).

#### References

- Adhikari B, Majumdar S. *Progress in Polymer Science* 2004;29(7):699–766.
- Ahuja T, Mir IA, Kumar D, Rajesh. *Biomaterials* 2007;28(5):791–805. [PubMed: 17055573]
- Arntz Y, Seelig JD, Lang HP, Zhang J, Hunziker P, Ramseyer JP, Meyer E, Hegner M, Gerber C. *Nanotechnology* 2003;14(1):86–90.
- Chua JH, Chee R-E, Agarwal A, Wong SM, Zhang G-J. *Analytical Chemistry* 2009;81(15):6266–6271. [PubMed: 20337397]
- Cotton TM, Schultz SG, Van Duyne RP. *Journal of the American Chemical Society* 1980;102(27):7960–7962.
- Darain F, Yager P, Gan KL, Tjin SC. *Biosensors and Bioelectronics* 2009;24(6):1744–1750. [PubMed: 18945609]

- de Winter RJ, Koster RW, Sturk A, Sanders GT. *Circulation* 1995;92(12):3401–3407. [PubMed: 8521560]
- Dong H, Cao X, Li CM, Hu W. *Biosensors and Bioelectronics* 2008;23(7):1055–1062. [PubMed: 18078745]
- Gao Z, Agarwal A, Trigg AD, Singh N, Fang C, Tung C-H, Fan Y, Buddharaju KD, Kong J. *Analytical Chemistry* 2007;79(9):3291–3297. [PubMed: 17407259]
- Gerard M, Chaubey A, Malhotra BD. *Biosensors and Bioelectronics* 2002;17(5):345–359. [PubMed: 11888724]
- Gooding JJ. *Small* 2006;2(3):313–315. [PubMed: 17193042]
- Hamm CW. *Circulation* 2001;104(13):1454–1456. [PubMed: 11571234]
- Ishii J, Wang J-h, Naruse H, Taga S, Kinoshita M, Kurokawa H, Iwase M, Kondo T, Nomura M, Nagamura Y, Watanabe Y, Hishida H, Tanaka T, Kawamura K. *Clin Chem* 1997;43(8):1372–1378. [PubMed: 9267316]
- Ishikawa FN, Chang H-K, Curreli M, Liao H-I, Olson CA, Chen P-C, Zhang R, Roberts RW, Sun R, Cote RJ, Thompson ME, Zhou C. *ACS Nano* 2009;3(5):1219–1224. [PubMed: 19422193]
- Kwon OS, Park SJ, Jang J. *Biomaterials* 2010;31(17):4740–4747. [PubMed: 20227108]
- Lee I, Il Park H, Park S, Kim MJ, Yun M. *Nano* 2008;3(2):75–82.
- Lin T-W, Hsieh P-J, Lin C-L, Fang Y-Y, Yang J-X, Tsai C-C, Chiang P-L, Pan C-Y, Chen Y-T. *Proceedings of the National Academy of Sciences* 2010;107(3):1047–1052.
- Luo X, Killard AJ, Morrin A, Smyth MR. *Analytica Chimica Acta* 2006;575(1):39–44. [PubMed: 17723569]
- Masson J-F, Battaglia TM, Khairallah P, Beaudoin S, Booksh KS. *Analytical Chemistry* 2006;79(2):612–619. [PubMed: 17222027]
- Muhammad-Tahir Z, Alocilja EC. *Biosensors and Bioelectronics* 2003;18(5–6):813–819. [PubMed: 12706596]
- Nyamsi Hendji AM, Jaffrezic-Renault N, Martelet C, Shul'ga AA, Dzydevich SV, Soldatkin AP, El'skaya AV. *Sensors and Actuators B: Chemical* 1994;21(2):123–129.
- Painter PC, Koenig JL. *Biopolymers* 1975;14(3):457–468. [PubMed: 1174675]
- Patolsky F, Zheng G, Lieber CM. *Analytical Chemistry* 2006;78(13):4260–4269. [PubMed: 16856252]
- Pomfret SJ, Adams PN, Comfort NP, Monkman AP. *Polymer* 2000;41(6):2265–2269.
- Ruben LN, Edwards BF, Rising J. *Cellular and Molecular Life Sciences* 1977;33(11):1522–1524.
- Sangodkar H, Sukeerthi S, Srinivasa RS, Lal R, Contractor AQ. *Analytical Chemistry* 1996;68(5):779–783.
- Tang J, Huang J, Su B, Chen H, Tang D. *Biochemical Engineering Journal* 2011;53(2):223–228.
- Tang X, Bansaruntip S, Nakayama N, Yenilmez E, Chang Y-I, Wang Q. *Nano Letters* 2006;6(8):1632–1636. [PubMed: 16895348]
- Wanekaya, Adam K, Chen W, Myung, Nosang V, Mulchandani A. *Electroanalysis* 2006;18(6):533–550.
- Wang WU, Chen C, Lin K-h, Fang Y, Lieber CM. *Proceedings of the National Academy of Sciences of the United States of America* 2005;102(9):3208–3212. [PubMed: 15716362]
- Yun M, Myung NV, Vasquez RP, Lee C, Menke E, Penner RM. *Nano Letters* 2004;4(3):419–422.
- Zhang C, Zhang Z, Yu B, Shi J, Zhang X. *Analytical Chemistry* 2001;74(1):96–99. [PubMed: 11795824]
- Zhang J, Liu C, Shi G. *Journal of Applied Polymer Science* 2005;96(3):732–739.



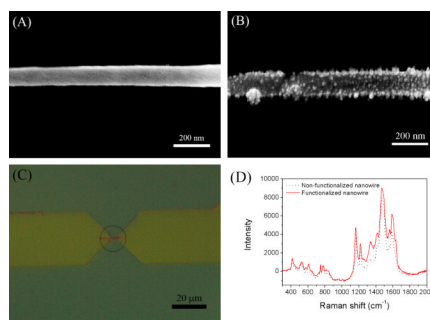


**Fig. 1.** (A) SEM image of non-functionalized single PANI nanowire. (B) SEM image of functionalized single PANI nanowire with IgG mAbs. (C) Functionalized single PANI nanowire with IgG mAbs labeled by Texas Red fluorescent materials (in circle). (D) The comparison of Raman spectra before functionalization and after functionalization of single PANI nanowire with IgG mAbs.

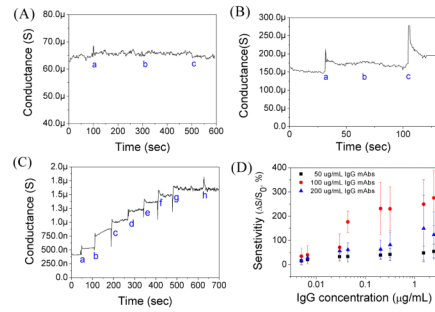


**Fig. 2.**

(A) Measurement of conductance changes on single non-functionalized PANI nanowire (a: PBS; b: BSA, 10  $\mu$ g/mL; and c: IgG, 3.3  $\mu$ g/mL). (B) Specificity test of functionalized single PANI nanowire with IgG mAbs (a: PBS; b: BSA, 50 ng/mL; and c: IgG, 33 ng/mL). (C) Detection of IgG on a single PANI nanowire biosensor (a: IgG, 5 ng/mL; b: IgG, 37 ng/mL; c: IgG, 54 ng/mL; d: IgG, 242 ng/mL; e: IgG, 368 ng/mL; f: IgG, 1.74  $\mu$ g/mL; g: IgG, 2.78  $\mu$ g/mL; and h: BSA, 5  $\mu$ g/mL). (D) Sensitivity of the single PANI nanowire biosensors with various concentrations of IgG mAbs (50, 100, and 200  $\mu$ g/mL).

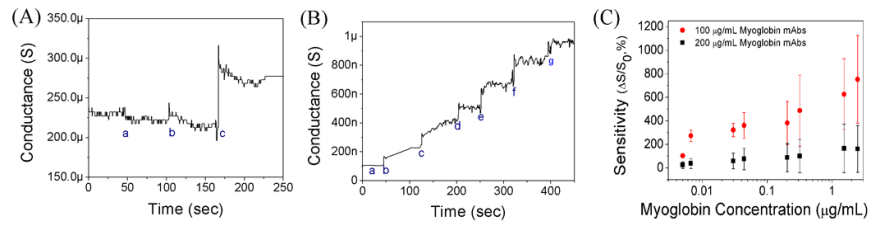


**Fig. 3.**

(A) Specificity and sensitivity of a single PANI nanowire biosensor for Myo (a: PBS; b: BSA, 500 ng/mL; and c: myoglobin, 1.4 ng/mL). (B) Detection of Myo on a single PANI nanowire biosensor (a: PBS, b: 5 ng/mL, c: 30 ng/mL, d: 50 ng/mL, e: 200 ng/mL, f: 350 ng/mL,  $\mu$  and g: 2.5  $\mu$ g/mL). (C) Sensitivity of single PANI nanowire biosensors with various concentrations of Myo mAbs (100 and 200  $\mu$ g/mL).